

## Supplemental Materials for Tuning lithium-yttrium chloride local dynamics through coordination control and mixing during synthesis

*Teerth Brahmhatt<sup>a,b</sup>, Cheng Li<sup>c</sup>, Mounesha N. Garaga<sup>d</sup>, Wan-Yu Tsai<sup>a</sup>, Steve G. Greenbaum<sup>d</sup>, Jagjit Nanda<sup>e</sup>, Robert L. Sacci<sup>a\*</sup>*

---

<sup>a</sup> Chemical Sciences Division, Oak Ridge National Laboratory, Oak Ridge, TN 38712 USA. E-mail: [saccir1@ornl.gov](mailto:saccir1@ornl.gov)

<sup>b</sup> Bredeesen Center for Interdisciplinary Research and Education, University of Tennessee, Knoxville, TN, 37996

<sup>c</sup> Neutron Scattering Division, Oak Ridge National Laboratory, Oak Ridge, TN 38712

<sup>d</sup> Department of Physics and Astronomy, Hunter College, City University of New York, New York, NY 10065

<sup>e</sup> Applied Energy Division, SLAC National Laboratory, Menlo Park, CA 94025

Larger high resolution images from manuscript are provided for the reader.

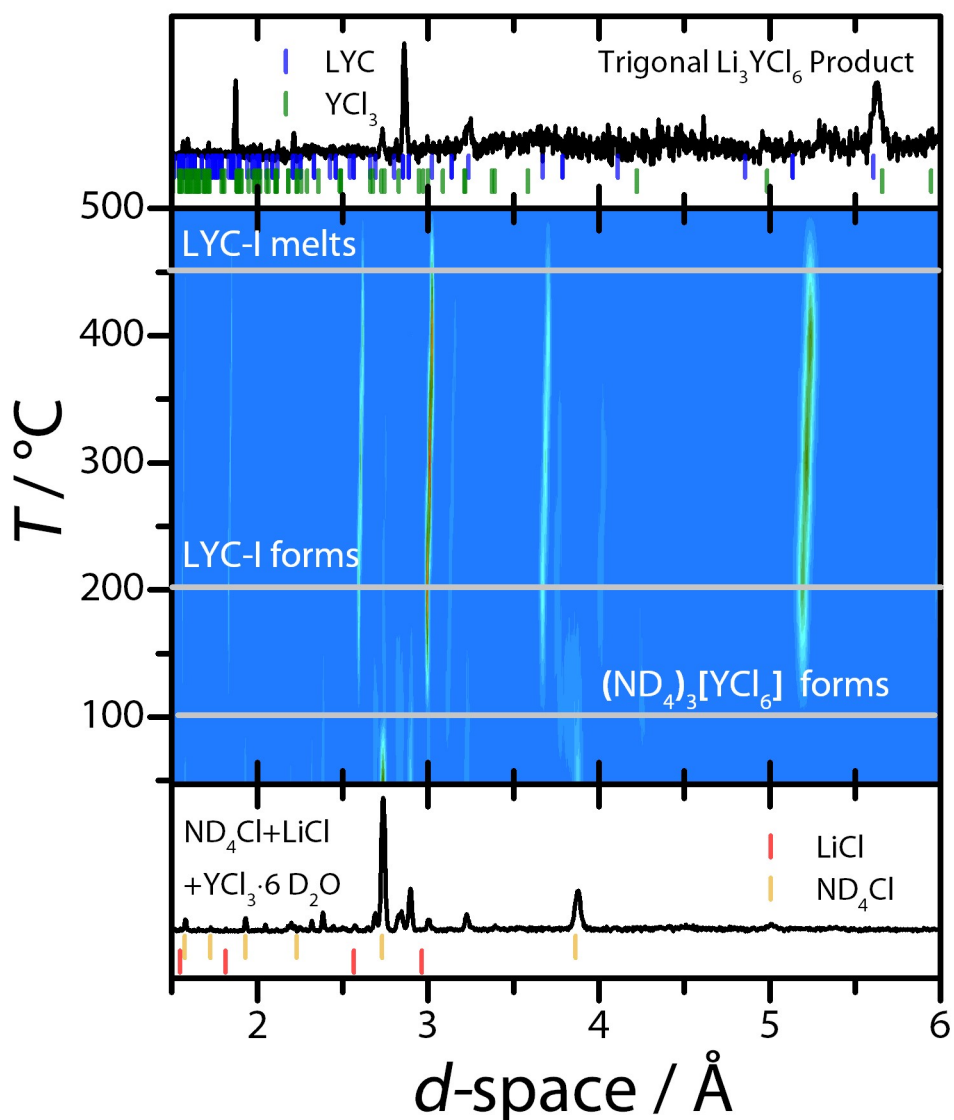


Figure S1: Visualization of the synthesis pathways using *in situ* neutron diffraction of the ammonium chloride-assisted synthesis from aqueous solution, heating from 47 to 500 °C. The initial NPD pattern is the precursors after dissolution and vacuum drying prior to ramping, the final NPD pattern is the RT product obtained after ramping and cooling.

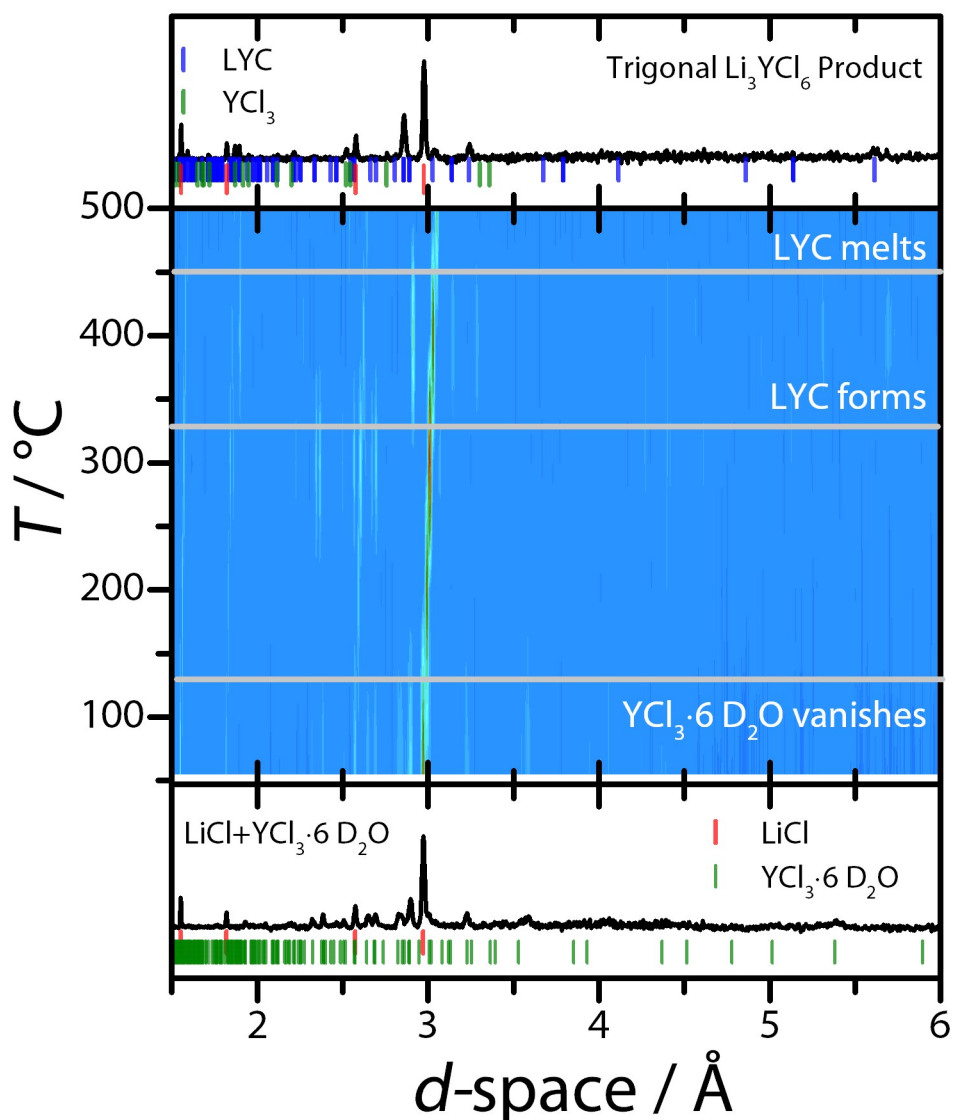


Figure S2: Visualization of the synthesis pathways using *in situ* neutron diffraction of the ammonium chloride-free synthesis from aqueous solution, heating from 45 to 500 °C. The initial NPD pattern is the precursors after dissolution and vacuum drying prior to ramping, the final NPD pattern is the RT product obtained after ramping and cooling.

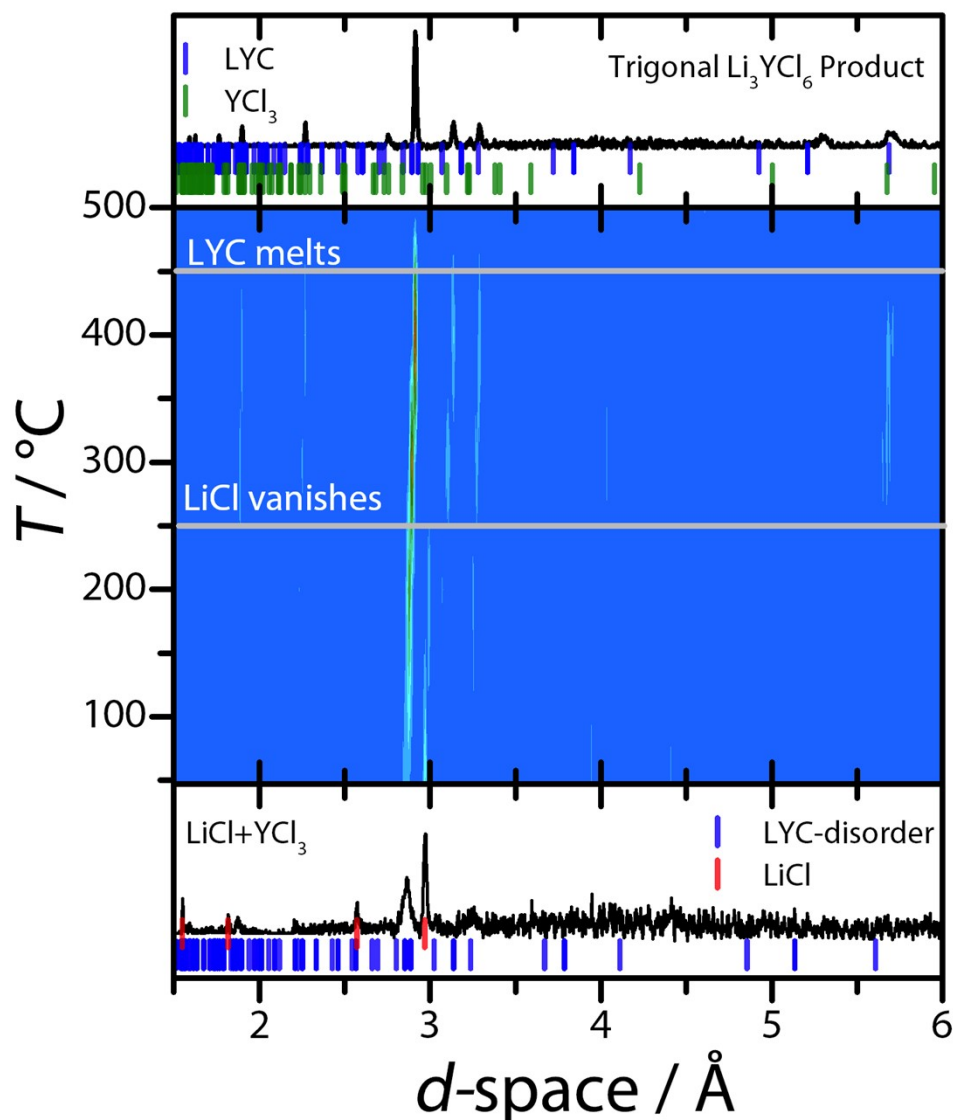


Figure S3: Visualization of the synthesis pathways using *in situ* neutron diffraction of the mechanochemical LYC synthesis, heating from 45 to 500  $^\circ\text{C}$ . The initial NPD pattern is the precursors after dissolution and vacuum drying prior to ramping, the final NPD pattern is the RT product obtained after ramping and cooling.

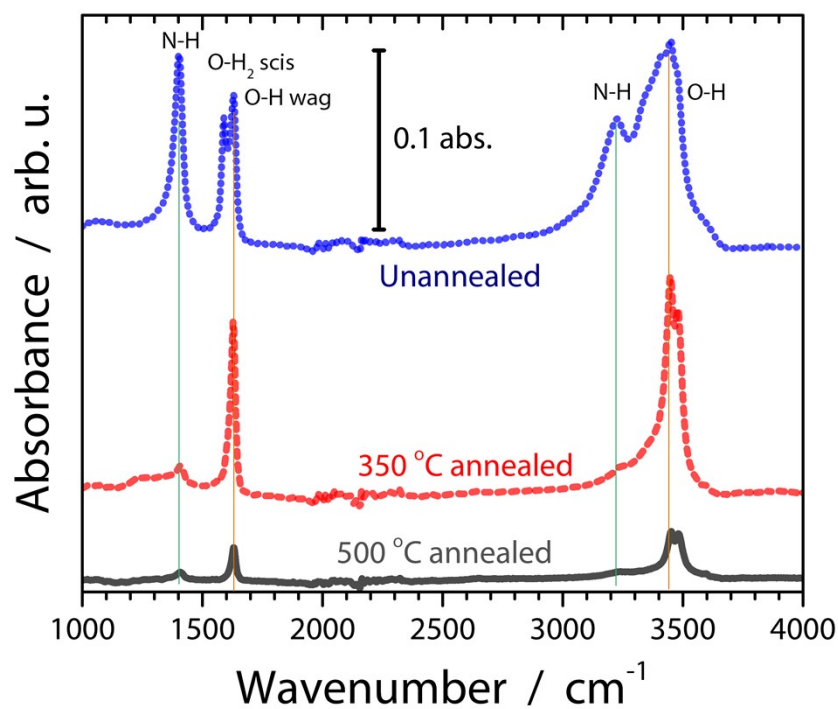


Figure S4: Infrared absorbance spectra of AC-LYC samples measured using a diamond crystal attenuated total reflection accessory at cut at a  $45^\circ$  angle. Absorbances are offset for clarity. Unannealed, as-dried, sample shows clear N-H bands, while annealing at  $350^\circ\text{C}$  leaves behind little N-H bands suggesting ammonium is removed. Further annealing at  $500^\circ\text{C}$  reduces strongly adsorbed  $\text{H}_2\text{O}$  and hydroxyl groups.



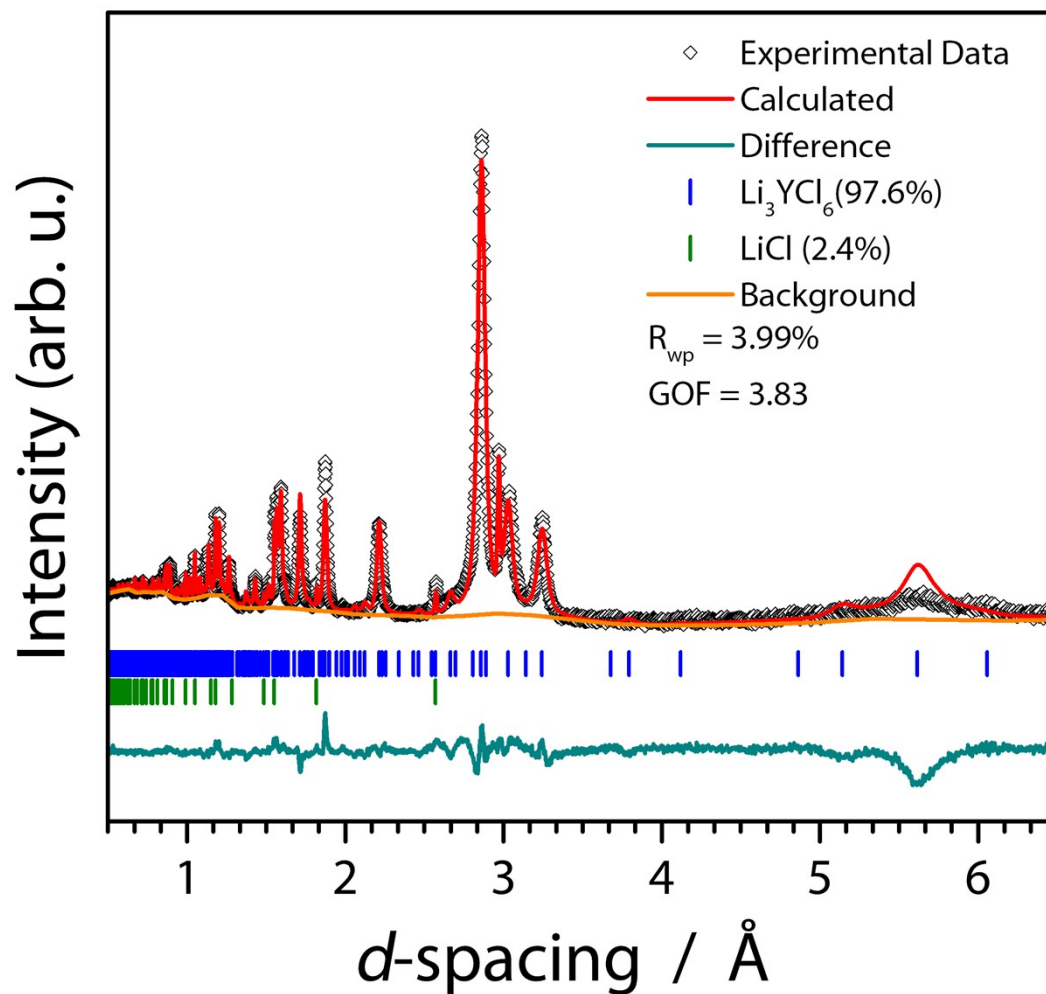
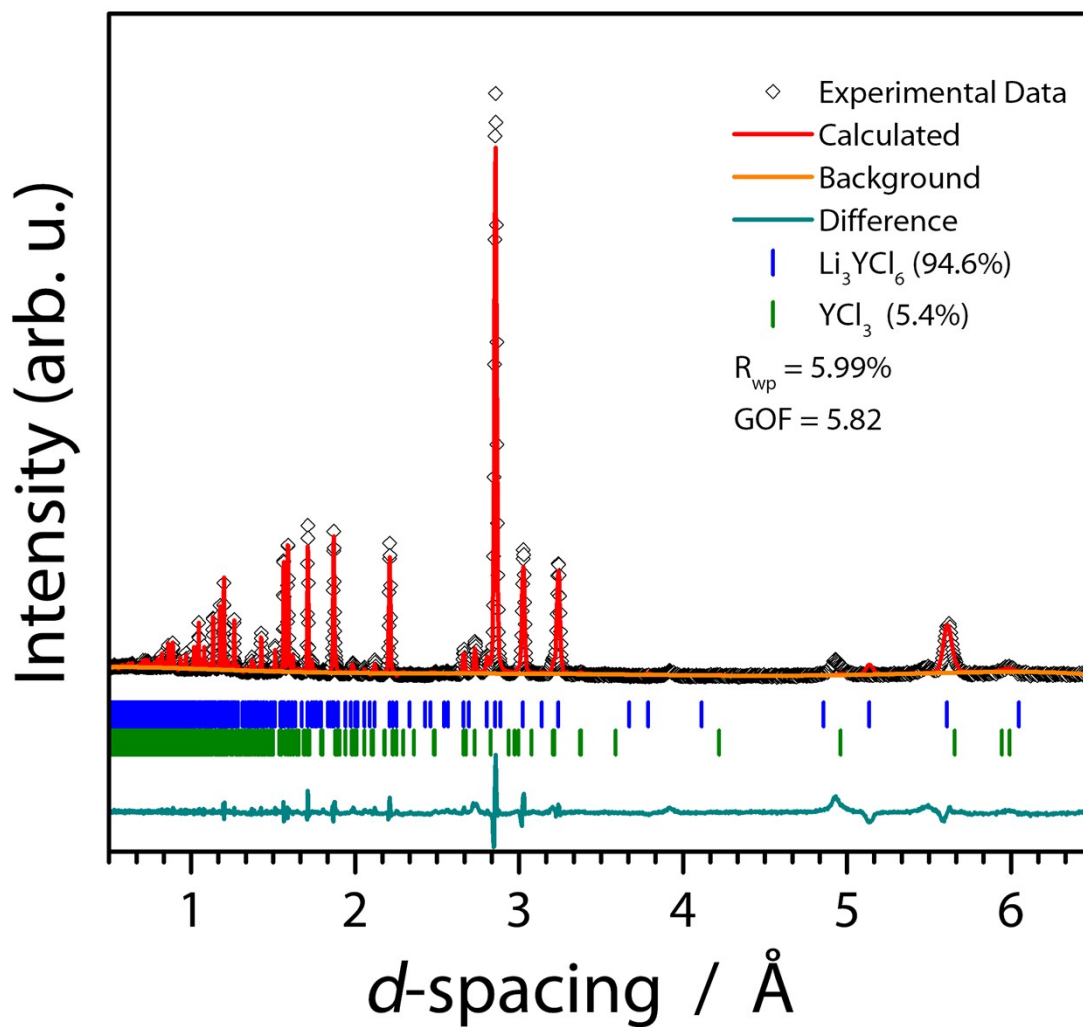


Figure S6: Refinement of the neutron powder diffraction data of the tetragonal LYC product synthesized through the mechanochemical route before annealing. This sample was synthesized in parallel to the *in situ* diffraction samples. Note, the non-flat background is indicative of an amorphous phase, presumably  $\text{YCl}_3$  as it is observed in the following figure.



Fi

Figure S7: Refinement of the neutron powder diffraction data of the tetragonal LYC product synthesized by annealing the mechanochemical sample shown in Figure S5. This sample was synthesized in parallel to the *in situ* diffraction samples.



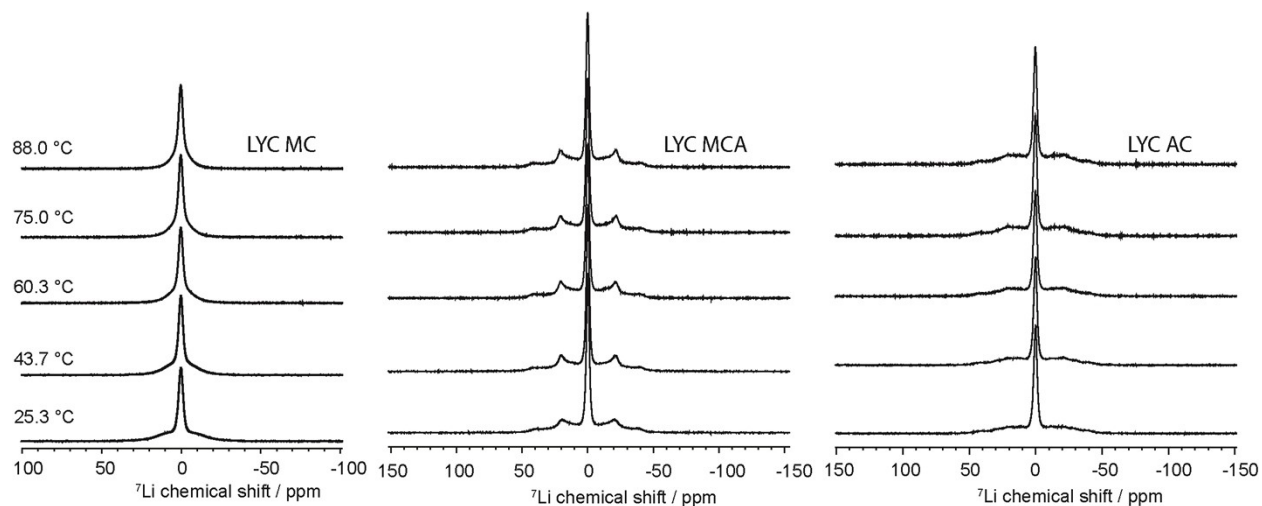


Figure S8:  ${}^7\text{Li}$  static NMR spectra of MC, MCA and AC samples as a function of temperature.

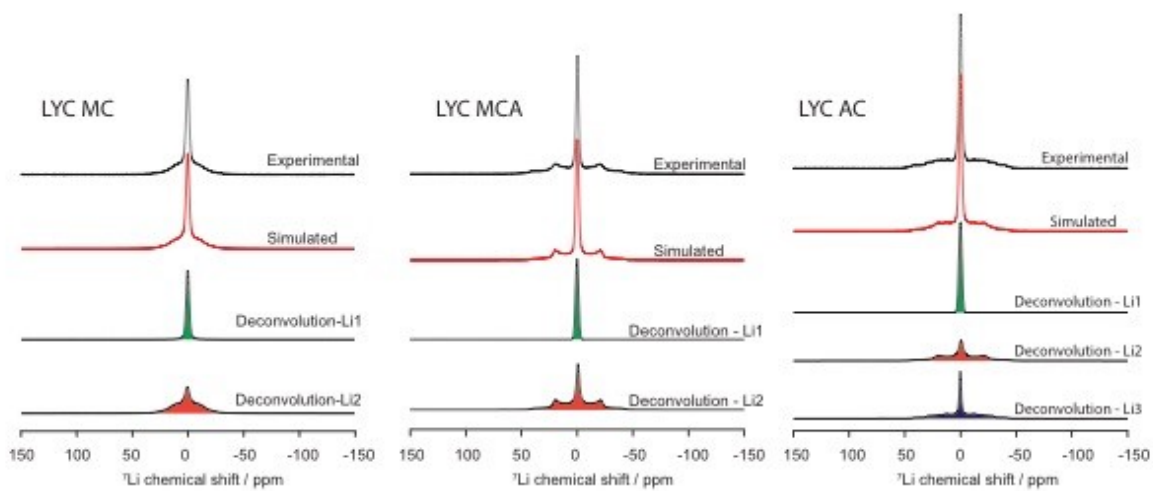


Figure S9: Representative deconvolution of the  ${}^7\text{Li}$  static NMR spectra of MC, MCA and AC.